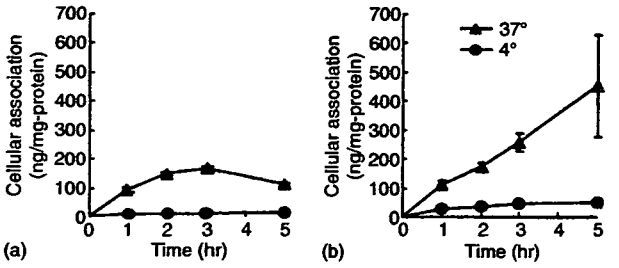

Figure 1. Cellular association time courses of naked [^{32}P]pDNA (a) or [^{32}P]pDNA/Lipofectin complex (b) in DC2.4 cells. Cells were incubated at 37° (closed triangle) or 4° (closed circle). Each point represents the mean ± SD (n = 3).

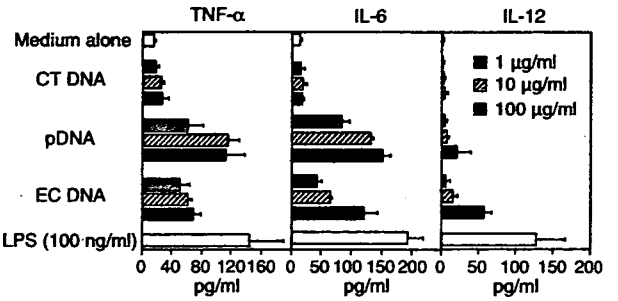

Figure 3. Cytokine secretion induced by naked DNA from GM-CSF DC. The cells were incubated with EC DNA, pDNA, or CT DNA for 8 hr. The supernatants were collected and the amount of TNF-α, IL-6, and IL-12 secreted from the cells was determined by ELISA. Each result represents the mean ± SD (n = 3).

uptake in DC2.4 cells and the amount of [^{32}P]pDNA increased in a time-dependent manner (Fig. 1b).

Next, we examined the localization of fluorescence-labelled DNA (FL-pDNA). In the confocal microscopy experiments, the fluorescence derived from naked FL-pDNA is bound to the cellular membrane at 4° (Fig. 2a). At 37°, FL-pDNA was observed inside the cells after 1 hr and it appeared to accumulate in the nucleus after a 3 hr incubation. On the other hand cationic lipids completely changed the localization of DNA. The fluorescence of the FL-pDNA/Lipofectin complex was observed in a punctuated pattern at 1 hr, then diffused into the cells after a 3 hr incubation (Fig. 2b).

The activation of GM-CSF DC by DNA

Next, cytokine production from DC by naked DNA was examined. Plasmid DNA and *E. coli* DNA were used as models of bacterial CpG DNA, and calf thymus DNA was used as a model of vertebrate DNA. As shown in Fig. 3, naked bacterial plasmid DNA and *E. coli* DNA with replete immunostimulatory CpG motifs induced TNF-α, IL-6 and IL-12 secretions from bone marrow-derived DC. The results are consistent with previous studies demonstrating that plasmid DNA stimulates GM-CSF DC to induce TNF-α and IL-12.[18] Vertebrate calf thymus DNA (CT DNA) containing less CpG motifs did not. LPS induced small amounts of cytokines, probably because of relatively short-term incubation (8 hr). Similar results were observed in the experiment using DC2.4 cells, although the cells released a higher amount of cytokines (Fig. 4). These results demonstrate that the cytokine secretion from the DC corresponds to the difference between endogenous DNA and exogenous DNA.

Next, cellular activation in DC by DNA/cationic lipid complexes was examined. The *E. coli* DNA/Lipofectin complexes stimulated GM-CSF cultured DC to produce cytokines, TNF-α, IL-6 and IL-12 in a dose-dependent manner (Fig. 5). Similar results were observed with pDNA/Lipofectin complex. The amounts of cytokines released from the DC were significantly increased by complex formation with cationic lipids compared with naked DNA (Fig. 3). The DC were unable to produce a significant amount of pro-inflammatory cytokines following

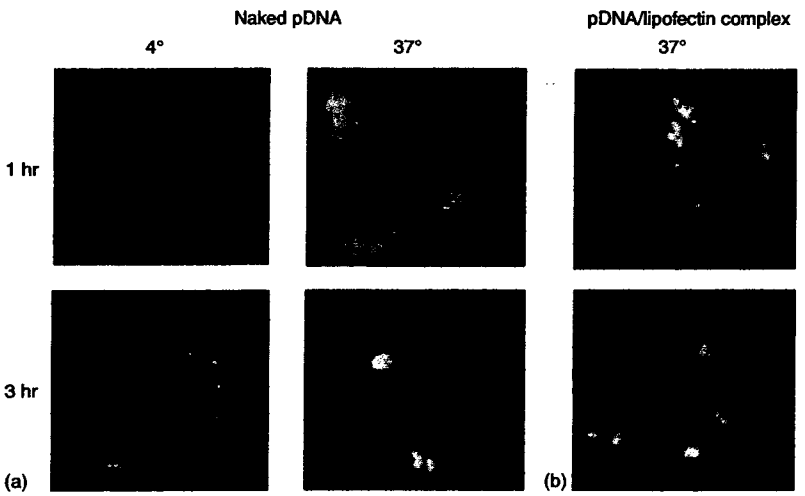

Figure 2. Uptake of naked FL-pDNA (a) or FL-pDNA/Lipofectin complex (b) by DC2.4 cells. The cells were incubated with 5·0 μg/ml naked FL-pDNA or 30 μg/ml FL-pDNA/Lipofectin complex.

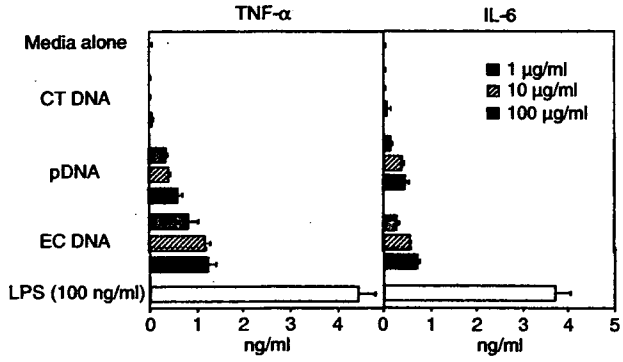

Figure 4. Cytokine secretion induced by naked DNA from DC2.4 cells. The cells were incubated with EC DNA, pDNA, or CT DNA for 8 hr. The supernatants were collected and the amount of TNF-α and IL-6 secreted from the cells was determined by ELISA. Each result represents the mean ± SD ($n = 3$).

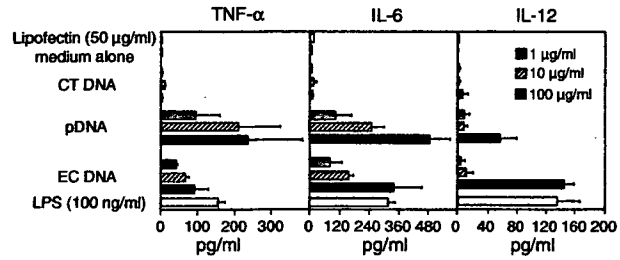

Figure 5. Cytokine secretion induced by DNA/Lipofectin complex from GM-CSF DC. The cells were incubated with EC DNA, pDNA, or CT DNA/Lipofectin complex (5 μl Lipofectin per 1 μg DNA). After a 2 hr incubation, liposomes were removed and fresh growth medium was added to the cells. The supernatants were collected 8 hr after the incubation with liposomes. The amount of TNF-α, IL-6, and IL-12 secreted from the cells was determined by ELISA. Each result represents the mean ± SD ($n = 3$).

stimulation with vertebrate calf thymus DNA (CT DNA) containing less CpG motifs when DNA is complexed to Lipofectin. Lipids alone were unable to stimulate the DC sufficiently to release pro-inflammatory cytokines. Similar results were obtained in DC2.4 cells (Fig. 6). These results demonstrate that GM-CSF DC discriminate between bacterial DNA and mammalian DNA.

Discussion

The most important role of immune system is to distinguish between 'self' and 'non-self'. Although the TLR9 subfamily (TLR7, 8 and 9) recognizes non-self nucleic acids[31] under special conditions, such as systemic lupus erythematosus, these TLRs are stimulated in response to self nucleic acids. For example chromatin–immunoglobulin complexes trigger DC activation in a TLR9-dependent and TLR9-independent manner.[32] Recently, Barton *et al.* have demonstrated that the fusion protein of

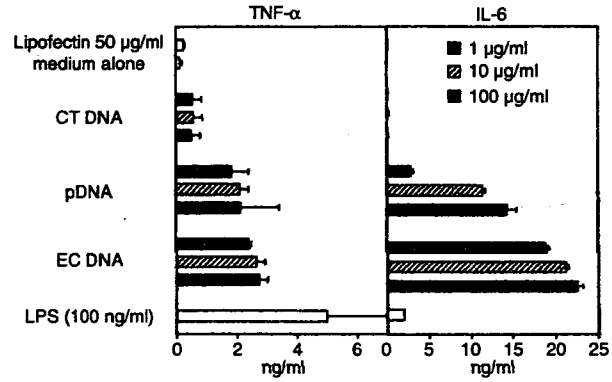

Figure 6. Cytokine secretion induced by DNA/Lipofectin complex from DC2.4 cells. The cells were incubated with EC DNA, pDNA, or CT DNA/Lipofectin complex (5 μl Lipofectin per 1 μg DNA). After a 2 hr incubation, liposomes were removed and fresh growth medium was added to the cells. The supernatants were collected 8 h after the incubation with liposomes. The amount of TNF-α and IL-6 secreted from the cells was determined by ELISA. Each result represents the mean ± SD ($n = 3$).

TLR4/9, which is delivered to cellular membranes, is activated by vertebrate DNA.[33] One proposed hypothesis is that compartmentalization of TLR9 prevents the response induced by endogenous DNA.

In the present study, we have demonstrated that GM-CSF-derived DC activation is triggered by exogenous naked DNA. Bacterial DNA induces cytokine secretion from DC, although vertebrate DNA does not. Flt-3 L cultured murine DC (Flt-3 L DC) also induce activation of TLR9 in response to naked bacterial DNA, but not naked vertebrate DNA.[24] Therefore, these studies imply that both GMCSF-DC and Flt-3 L DC can discriminate between bacterial non-self DNA and vertebrate self DNA.

On the other hand, these characteristics are different from murine macrophages.[22] Primary macrophages do not respond to naked DNA in spite of TLR9 expression, although the macrophage-like cell line RAW264.7 cells do. Both primary macrophages and DC take up DNA via a similar mechanism.[15–17] The mechanism of unresponsiveness of macrophages to DNA has not been elucidated, although TLR9 is present in the cells. Macrophages have deoxyribonuclease II (DNase II) in the lysosomal compartment, and they are responsible for apoptotic cell engulfment, DNA digestion and erythroid cell differentiation.[34] In erythropoiesis, macrophages take up nuclei and digest DNA. In DNase II-deficient mice, undigested DNA in macrophages causes IFN-β production via unknown receptors.[35] The cytokine production is mediated by the TLR9/MyD88 pathway and novel pathways that have been identified recently.[36,37] Therefore, the mechanism of the unresponsiveness of macrophages to naked DNA may involve the limited uptake and degradation by DNase II. However, further investigation is required.

The TLR4/9 fusion protein on the cell membrane is activated by vertebrate DNA.[33] This research indicates that compartmentalization into cells avoids TLR9 responses to endogenous DNA. Therefore, we forced DNA to internalize into cells using cationic lipids. In fact, vertebrate DNA/cationic lipid complexes can induce cytokine secretion from murine macrophages and Flt-3 L DC.[23,24] Following enhancement of DNA uptake by cationic lipids, these cells cannot distinguish between 'self' and 'non-self' DNA. In peritoneal macrophages, complexation of calf thymus DNA with cationic lipids elicited a similar level of inflammatory cytokine production to that obtained with bacterial *E. coli* DNA using cationic lipids.[23] In addition, calf thymus DNA with cationic lipid DOTAP causes a high degree of IFN-α release from murine Flt-3 L cultured DC or human peripheral blood mononuclear cells.[24] The amount of IFN-α induced by calf thymus DNA with DOTAP is similar to that induced by bacterial plasmid DNA. However, the result with GM-CSF DC is different from that in these cells. The cells only recognize bacterial DNA. Vertebrate DNA/cationic lipid complexes do not stimulate GM-CSF DC, although bacterial DNA does. There are two possibilities to explain these observations. One is the possibility that different types of cationic lipids lead to different forms of delivery of DNA, and result in different responses. For example, murine macrophages release inflammatory cytokines in response to the addition of vertebrate CT DNA/cationic lipid complexes.[23] Lipofectamine was used for this research. Synthetic double-stranded DNA containing no CpG motif can stimulate macrophage cell lines when DNA is complexed with the cationic lipid Fugene 6.[38] In addition, vertebrate CT DNA/cationic lipid Lipofectamine complexes induce macrophage activation via TLR9-dependent and -independent mechanisms.[39] Flt-3 L cultured DC (Flt-3 L DC) also responds to vertebrate DNA/cationic lipid DOTAP complexes via TLR9-dependent and -independent pathways.[24] TLR9-independent activation is also observed following transfection using Lipofectamine 2000.[37] Honda *et al.* showed that different cellular distributions of DNA result in different cytokine responses.[40] CpG-B ODN normally do not induce IFN-α release from plasmacytoid DC. However, following complexation with DOTAP, the same ODNs trigger IFN-α. Confocal microscopy reveals that DOTAP retains DNA in early endosomes, although ODNs without DOTAP are immediately transferred to lysosomal vesicles. Taken together, enhancement of the DNA uptake may not explain the response of TLR9 to vertebrate DNA and TLR9 may be present in specific compartments.

The other possibility is that GM-CSF DC, Flt-3 L DC and macrophages may contribute to the immune systems in different ways, by producing different types or degrees of induction. TLR9 is mainly expressed in B cells and plasmacytoid DC in humans.[31] On the other hand, mouse TLR9 is also present in myeloid DC and macrophages. Although further studies are required to clarify the contribution of DC or macrophages to immune responses *in vivo*, the present study suggests that DC are the main cells that respond to naked bacterial DNA, although both DC and macrophages will release inflammatory cytokines after the administration of bacterial DNA/cationic lipid complexes.

Very recently Martin *et al.* have shown that GM-CSF DC release type I IFN upon stimulation of mammalian DNA complexed with Fugene, another kind of lipid for transfection.[41] Interestingly, the cells do not produce TNF-α, IL-6 or IL-12. The activation is independent of TLR9 because GM-CSF DC from TLR9$^{-/-}$ deficient mice respond to mammalian DNA/Fugene complexes to secrete type I IFN. Another group has also demonstrated that non-CpG DNA/lipofectamine complexes stimulate GM-CSF DC to induce type I IFN.[42] The activation is not dependent on the MyD88 or TRIF pathways. Based on these observations, one can hypothesize that, distinct from Flt-3 L DC, GM-CSF DC respond to only bacterial or viral DNA via TLR9-dependent pathway, and release cytokines, such as TNF-α IL-6 and IL-12. However when mammalian DNAs are translocated into cells, GM-CSF DC may not induce these cytokines. Instead, the cells may release IFN-α through a TLR9-independent pathway. Further studies are required for these TLR9-dependent and -independent mechanisms.

In conclusion, the present study has demonstrated that murine GM-CSF DC or the DC cell line, DC2.4, produce pro-inflammatory cytokines following stimulation with CpG-containing DNAs and this production is increased when the DNAs are added to the cells in a complex form with cationic lipids. These findings form an important basis for future DNA-based therapies, including gene therapy and DNA vaccination.

Acknowledgements

This work was supported in part by 21st Century COE Program 'Knowledge Information Infrastructure for Genome Science', and also in part by a grant-in-aid for Scientific Research from the Ministry of Education, Culture, Sports, Science and Technology, Japan. We would like to thank Dr Kenneth Rock (Department of Pathology, University of Massachusetts Medical School, MA, USA) for providing DC2.4 cells.

References

1 Krieg AM. CpG motifs in bacterial DNA and their immune effects. *Annu Rev Immunol* 2002; **20**:709–60.

2 Yasuda K, Wagner H, Takakura Y. Role of immunostimulatory DNA and TLR9 in gene therapy. *Crit Rev Ther Drug Carrier Syst* 2006; **23**:89–110.

3 Haddad EB, Rousell J, Lindsay MA, Barnes PJ. Synergy between tumor necrosis factor alpha and interleukin 1beta in inducing transcriptional down-regulation of muscarinic M2 receptor gene expression. Involvement of protein kinase A and ceramide pathways. *J Biol Chem* 1996; **271**:32586–92.

4 Qin L, Ding Y, Pahud DR, Chang E, Imperiale MJ, Bromberg JS. Promoter attenuation in gene therapy. interferon-gamma and tumor necrosis factor-alpha inhibit transgene expression. *Hum Gene Ther* 1997; **8**:2019–29.

5 Sellins K, Fradkin L, Liggitt D, Dow S. Type I Interferons potently suppress gene expression following gene delivery using liposome (–) DNA complexes. *Mol Ther* 2005; **12**:451–9.

6 Gurunathan S, Klinman DM, Seder RADNA vaccines: immunology, application, and optimization. *Annu Rev Immunol* 2000; **18**:927–74.

7 Raz E, Tighe H, Sato Y *et al.* Preferential induction of a Th1 immune response and inhibition of specific IgE antibody formation by plasmid DNA immunization. *Proc Natl Acad Sci USA* 1996; **93**:5141–5.

8 Roman M, Martin OE, Goodman JS *et al.* Immunostimulatory DNA sequences function as T helper-1-promoting adjuvants. *Nat Med* 1997; **3**:849–54.

9 Seder RA, Hill AV. Vaccines against intracellular infections requiring cellular immunity. *Nature* 2000; **406**:793–8.

10 Steinman RM, Dhodapkar M. Active immunization against cancer with dendritic cells: the near future. *Int J Cancer* 2001; **94**:459–73.

11 Kadowaki N, Antonenko S, Liu YJ. Distinct CpG DNA and polyinosinic-polycytidylic acid double-stranded RNA, respectively, stimulate CD11c (–) type 2 dendritic cell precursors and CD11c (+) dendritic cells to produce type I IFN. *J Immunol* 2001; **166**:2291–5.

12 Weiner GJ. The immunobiology and clinical potential of immunostimulatory CpG oligodeoxynucleotides. *J Leukoc Biol* 2000; **68**:455–63.

13 Ahmad-Nejad P, Hacker H, Rutz M, Bauer S, Vabulas RM, Wagner H. Bacterial CpG-DNA and lipopolysaccharides activate Toll-like receptors at distinct cellular compartments. *Eur J Immunol* 2002; **32**:1958–68.

14 Latz E, Schoenemeyer A, Visintin A *et al.* TLR9 signals after translocating from the ER to CpG DNA in the lysosome. *Nat Immunol* 2004; **5**:190–8.

15 Yoshinaga T, Yasuda K, Ogawa Y, Takakura Y. Efficient uptake and rapid degradation of plasmid DNA by murine dendritic cells via a specific mechanism. *Biochem Biophys Res Commun* 2002; **299**:389–94.

16 Takagi T, Hashiguchi M, Mahato RI, Tokuda H, Takakura Y, Hashida M. Involvement of specific mechanism in plasmid DNA uptake by mouse peritoneal macrophages. *Biochem Biophys Res Commun* 1998; **245**:729–33.

17 Takakura Y, Takagi T, Hashiguchi M *et al.* Characterization of plasmid DNA binding and uptake by peritoneal macrophages from class A scavenger receptor knockout mice. *Pharm Res* 1999; **16**:503–8.

18 Hacker H, Mischak M, Miethke T *et al.* CpG-DNA-specific activation of antigen-presenting cells requires stress kinase activity and is preceded by non-specific endocytosis and endosomal maturation. *EMBO J* 1998; **17**:6230–40.

19 Yi AK, Tuetken R, Redford T, Waldschmidt M, Kirsch J, Krieg AM. CpG motifs in bacterial DNA activate leukocytes through the pH-dependent generation of reactive oxygen species. *J Immunol* 1998; **160**:4755–61.

20 Hemmi H, Takeuchi O, Kawai T *et al.* A Toll-like receptor recognizes bacterial DNA. *Nature* 2000; **408**:740–5.

21 Honda K, Yanai H, Mizutani T *et al.* Role of a transductional-transcriptional processor complex involving MyD88 and IRF-7 in Toll-like receptor signaling. *Proc Natl Acad Sci USA* 2004; **101**:15416–21.

22 Yasuda K, Kawano H, Yamane I, Ogawa Y, Yoshinaga T, Nishikawa M, Takakura Y. Restricted cytokine production from mouse peritoneal macrophages in culture in spite of extensive uptake of plasmid DNA. *Immunology* 2004; **111**:282–90.

23 Yasuda K, Ogawa Y, Kishimoto M, Takagi T, Hashida M, Takakura Y. Plasmid DNA activates murine macrophages to induce inflammatory cytokines in a CpG motif-independent manner by complex formation with cationic liposomes. *Biochem Biophys Res Commun* 2002; **293**:344–8.

24 Yasuda KYuP, Kirschning CJ *et al.* Endosomal translocation of vertebrate DNA activates dendritic cells via TLR9-dependent and -independent pathways. *J Immunol* 2005; **174**:6129–36.

25 Yasuda K, Rutz M, Schlatter B *et al.* CpG motif-independent activation of TLR9 upon endosomal translocation of 'natural' phosphodiester DNA. *Eur J Immunol* 2006; **36**:431–6.

26 Shen Z, Reznikoff G, Dranoff G, Rock KL. Cloned dendritic cells can present exogenous antigens on both MHC class I and class II molecules. *J Immunol* 1997; **158**:2723–30.

27 Nomura T, Yasuda K, Yamada T, Okamoto S, Mahato RI, Watanabe Y, Takakura Y, Hashida M. Gene expression and antitumor effects following direct interferon (IFN)-gamma gene transfer with naked plasmid DNA and DC-chol liposome complexes in mice. *Gene Ther* 1999; **6**:121–9.

28 Sambrook J, Fritsch EF, Maniatis T *Molecular Cloning: a Laboratory Manual*, 2nd edn. Cold Spring Harbor, NY: Cold Spring. Harbor Laboratory Press, 1989.

29 Cotten M, Baker A, Saltik M, Wagner E, Buschle M. Lipopolysaccharide is a frequent contaminant of plasmid DNA preparations and can be toxic to primary human cells in the presence of adenovirus. *Gene Ther* 1994; **1**:239–46.

30 Hartmann G, Krieg AM. CpG DNA and LPS induce distinct patterns of activation in human monocytes. *Gene Ther* 1999; **6**:893–903.

31 Wagner H. The immunobiology of the TLR9 subfamily. *Trends Immunol* 2004; **25**:381–6.

32 Boule MW, Broughton C, Mackay F, Akira S, Marshak-Rothstein A, Rifkin IR. Toll-like receptor 9-dependent and -independent dendritic cell activation by chromatin-immunoglobulin G complexes. *J Exp Med* 2004; **199**:1631–40.

33 Barton GM, Kagan JC, Medzhitov R. Intracellular localization of Toll-like receptor 9 prevents recognition of self DNA but facilitates access to viral DNA. *Nat Immunol* 2006; **7**:49–56.

34 Nagata S. DNA degradation in development and programmed cell death. *Annu Rev Immunol* 2005; **23**:853–75.

35 Yoshida H, Okabe Y, Kawane K, Fukuyama H, Nagata S. Lethal anemia caused by interferon-beta produced in mouse embryos carrying undigested DNA. *Nat Immunol* 2005; **6**:49–56.

36 Okabe Y, Kawane K, Akira S, Taniguchi T, Nagata S. Toll-like receptor-independent gene induction program activated by

mammalian DNA escaped from apoptotic DNA degradation. *J Exp Med* 2005; **202**:1333–9.

37 Ishii KJ, Coban C, Kato H *et al.* A Toll-like receptor-independent antiviral response induced by double-stranded B-form DNA. *Nat Immunol* 2006; **7**:40–8.

38 Zhu FG, Reich CF, Pisetsky DS. Effect of cytofectins on the immune response of murine macrophages to mammalian DNA. *Immunology* 2003; **109**:255–62.

39 Yasuda K, Ogawa Y, Yamane I, Nishikawa M, Takakura Y. Macrophage activation by a DNA/cationic liposome complex requires endosomal acidification and TLR9-dependent and -independent pathways. *J Leukoc Biol* 2005; **77**:71–9.

40 Honda K, Ohba Y, Yanai H, Negishi H, Mizutani T, Takaoka A, Taya C, Taniguchi T. Spatiotemporal regulation of MyD88-IRF-7 signaling for robust type-I interferon induction. *Nature* 2005; **434**:1035–40.

41 Martin DA, Elkon KB. Intracellular mammalian DNA stimulates myeloid dendritic cells to produce type I interferons predominantly through a toll-like receptor 9-independent pathway. *Arthritis Rheum* 2006; **54**:951–60.

42 Stetson DB, Medzhitov R. Recognition of cytosolic DNA activates an IRF3-dependent innate immune response. *Immunity* 2006; **24**:93–103.

Title: Potential relevance of cytoplasmic viral sensors and related regulators involving innate immunity in antiviral response

Short title: Innate immunity and therapeutic response

Authors: Yasuhiro Asahina, M.D.[1], Namiki Izumi, M.D.[1], Itsuko Hirayama, M.D.[1], Tomohiro Tanaka, M.D.[1], Mitsuaki Sato, M.D.[1,2], Yutaka Yasui, M.D. [1], Nobutoshi Komatsu, M.D.[1,2], Naoki Umeda, M.D.[1], Takanori Hosokawa, M.D.[1], Ken Ueda, M.D.[1], Kaoru Tsuchiya, M.D.[1], Hiroyuki Nakanishi, M.D.[1], Jun Itakura, M.D.[1], Masayuki Kurosaki, M.D.[1], Nobuyuki Enomoto, M.D.[2], Megumi Tasaka, M.D. [3], Naoya Sakamoto, M.D. [3] and Shozo Miyake, M.D.[1]

[1] Department of Gastroenterology and Hepatology, Musashino Red Cross Hospital, 1-26-1 Kyonan-cho, Musashino-shi, Tokyo 180-8610, Japan

[2] First Department of Internal Medicine, Faculty of Medicine, University of Yamanashi, 1110 Shimogato, Chuo-shi, Yamanashi 409-3898, Japan

[3] Department of Gastroenterology and Hepatology, Tokyo Medical and Dental University, 1-5-45 Yushima, Bunkyo-ku, Tokyo 113-8519, Japan

Grant support: This study was supported by grants from the Miyakawa Memorial Research Foundation; the Japanese Ministry of Education, Culture, Sports, Science and

Technology; and the Japanese Ministry of Welfare, Health and Labor.

Abbreviations: HCV, hepatitis C virus; PEG-IFN, pegylated interferon; NVR, non-virological responders; RIG-I, retinoic acid-inducible gene I; MDA5, melanoma differentiation associated gene 5; CARD, Caspase-recruiting domain; Cardif, caspase-recruiting domain adaptor inducing IFN-beta; IPS-1, IFN-beta promoter stimulator I; MAVS, mitochondrial antiviral signaling protein; VISA, virus-induced signaling adaptor; RNF125, ring-finger protein 125; ISG15, IFN-stimulated gene 15; USP18, ubiquitin-specific protease 18; UBP43, ubiquitin-specific protease 43; G3PDH, glyceraldehyde-3-phosphate dehydrogenase; HMBS, hydroxymethylbilane synthase; PBMC, peripheral blood mononuclear cell; SVR, sustained viral responder; TR, transient responder; ROC, receiver operator characteristic; JAK, Janus kinase.

Correspondence:

Namiki Izumi M.D., Ph.D.

Chief, Department of Gastroenterology and Hepatology

Musashino Red Cross Hospital

1-26-1 Kyonan-cho, Musashino-shi

Tokyo 180-8610, Japan

Tel: +81-422-32-3111

Fax: +81-422-32-9551

E-mail address: nizumi@musashino.jrc.or.jp

Financial Disclosures: The authors who participated in this study have had no affiliation with the manufacturers of the drugs involved either in the past or in present, and have not received funding from the manufacturers to conduct this research.

ABSTRACT

Background & Aim: Clinical significance of molecules involving innate immunity in treatment response remains unclear. The aim is to elucidate the mechanisms underlying resistance to antiviral therapy and predictive usefulness of gene quantification in chronic hepatitis C (CH-C). ***Methods:*** We conducted a human study in 74 CH-C patients treated with PEG-IFN alpha-2b and ribavirin and 5 non-viral control patients. Expression of viral sensors, adaptor molecule, related ubiquitin E3-ligase, and modulators were quantified. ***Results:*** Hepatic RIG-I, MDA5, LGP2, ISG15 and USP18 in CH-C patients were up-regulated at 2- to 8-fold compared with non-HCV patients with a relatively constitutive Cardif. Hepatic RIG-I, MDA5, and LGP2 were significantly up-regulated in non-virological responders (NVR) compared with transient (TR) or sustained virological responders (SVR). Cardif and RNF125 were negatively correlated with RIG-I and significantly suppressed in NVR. Differences among clinical responses in RIG-I/Cardif and RIG-I/RNF125 ratio were conspicuous (NVR:TR:SVR = 1.3:0.6:0.4 and 2.3:1.3:0.8, respectively). Like viral sensors, ISG15 and USP18 were significantly up-regulated in NVR (4-fold and 2.3-fold, respectively). Multivariate and ROC analyses revealed higher RIG-I/Cardif ratio, ISG15, and USP18 predicted NVR. Lower Cardif in NVR was confirmed by its protein level in Western blot. Also, transcriptional responses in PBMC to the therapy were rapid and strong except for Cardif in not only positive (RIG-I, ISG15 and USP18) but also in negative regulatory manner (RNF125).

Conclusion: NVR may have adopted a different equilibrium in their innate immune response. High RIG-I/Cardif and RIG-I/RNF125 ratios, and ISG15 and USP18 are useful in identifying NVR.

Infection with hepatitis C virus (HCV) is a common cause of chronic hepatitis, which progresses to liver cirrhosis and hepatocellular carcinoma in many patients (1). Although combination therapy with pegylated interferon (PEG-IFN) alpha and ribavirin is now established as the standard treatment for chronic HCV infection genotype 1b, the sustained virological response rate in these patients is still around 50% (2–4). Moreover, physicians have also found that 20% of patients are non-virological responders (NVR; those whose HCV-RNA does not become negative during 48 weeks of combination therapy) (5). Prediction of NVR status is of clinical importance, because these patients have no chance of achieving a sustained virological response even after prolonged combination therapy (6). However, mechanisms involving resistance to PEG-IFN alpha and ribavirin have not been fully elucidated, and it is difficult to predict treatment responses before initiation of PEG-IFN alpha and ribavirin combination therapy.

In vitro studies have suggested that an innate immune response in viral infection is an essential part of the host antiviral defense system (7). HCV evades the host immune response through a complex combination of processes that include signaling interference, effector modulation, and continual viral genetic variation (8). We hypothesized that liver tissue would show a consistent difference between responders and non-responders in expression levels of the gene involved in innate immunity and IFN signal transduction. These differences could be used to predict treatment outcomes.

The retinoic acid-inducible gene I (RIG-I), a cytoplasmic RNA helicase, and the related melanoma differentiation associated gene 5 (MDA5) play essential roles in initiating the host antiviral response by detecting intracellular viral dsRNA (9–11). Caspase-recruiting

domain (CARD) adaptor inducing IFN-beta (Cardif), also called IFN-beta promoter stimulator 1 (IPS-1), mitochondrial antiviral signaling protein (MAVS), and virus-induced signaling adaptor (VISA), is an adaptor molecule. Cardif connects RIG-I sensing to downstream signaling, resulting in IFN beta gene activation (12–15). On the other hand, RIG-I sensing has been shown to be negatively regulated in a dominant-negative manner by LGP2 (10, 16), a helicase related to RIG-I and MDA5 lacking CARD. Interestingly, the ubiquitin ligase ring-finger protein 125 (RNF125) has been recently shown to conjugate ubiquitin to RIG-I, MDA5 as well as Cardif, which results in suppressing the functions of these proteins (17). Further, these molecules are ISGylated by IFN-stimulated gene 15 (ISG15), a ubiquitin-like protein (18), and ISG15 is specifically removed from ISGylated protein by ubiquitin-specific protease 18 (USP18), also called ubiquitin-specific protease 43 (UBP43) (19, 20). Moreover, the NS3/4A protease of HCV specifically cleaves Cardif as part of its immune evasion strategy (12, 21). Therefore, the RIG-I/Cardif system and its regulatory systems have essential key functions in the innate antiviral response (Supplemental Figure 1). However, the clinical significance of these innate immune systems, especially in relevance to the treatment response, is unclear, because findings in this field have been mainly obtained by in vitro experiments using cell lines.

The aim of this study was to elucidate the mechanisms underlying resistance to antiviral therapy in the clinical setting, and to determine whether quantification of transcripts of positive and negative cytoplasmic viral sensors and related regulatory molecules involving innate immune system is useful in predicting responses to PEG-IFN alpha and ribavirin combination therapy.

MATERIALS AND METHODS

Patients

Among patients with biopsy-proven chronic hepatitis C hospitalized at the Musashino Red Cross Hospital, 74 patients of HCV genotype 1b with a high viral load (>100 KIU/mL by Amplicor-HCV Monitor Assay; Roche Molecular Diagnostics Co., Tokyo, Japan) were included in the present study (Table 1). Patients with liver cirrhosis, autoimmune hepatitis, or alcoholic liver injury were excluded. No patient was positive for hepatitis B virus-associated antigen/antibody or anti-human immunodeficiency virus antibody. No patient received immunomodulatory therapy prior to the enrollment. Written informed consent was obtained from all the patients, and this study was approved by the ethical committee of Musashino Red Cross Hospital in accordance with the Helsinki Declaration. Five patients with non-viral liver disease (two had autoimmune hepatitis and three had primary biliary cirrhosis) were included in the present study as controls.

Treatment protocol

The patients were treated for 48 weeks with subcutaneous injections of PEG-IFN alpha-2b (PegIntron®, Schering-Plough Corporation, Kenilworth, NJ, USA) at a dose of 1.5 $\mu g\ kg^{-1}\ week^{-1}$. Ribavirin (Rebetol®, Schering-Plough Corporation) was administered concomitantly over the 48-week period, given orally twice daily at a total daily dose of 600 mg for the patients who weighed less than 60 kg and 800 mg for the patients who weighed between 60 and 80 kg. The dose of PEG-IFN alpha-2b was

reduced to 0.75 μg kg^{-1} $week^{-1}$ when either the neutrophil count was <750/mm^3 or the platelet count was <80 × 10^3/mm^3. The dose of ribavirin was reduced to 600 mg/day when the hemoglobin concentration decreased to <10 g/dL.

Measurement of gene expression in the liver

Liver biopsy was performed immediately before starting the therapy. After extraction of total RNA from liver biopsy specimens, the mRNA expression of positive and negative cytoplasmic viral sensors (RIG-I, MDA5, and LGP2), the adaptor molecule (Cardif), related ubiquitin E3-ligase (RNF125), and the modulators of these molecules (ISG15 and USP18) was quantified by real-time quantitative PCR using primers specific for target genes. In brief, total RNA was extracted by the acid-guanidium–phenol–chloroform method using Isogen (Nippon Gene Co. Ltd., Toyama, Japan) from the liver biopsy specimen, which was 0.2–0.4 cm in length and 13 gauge in diameter. cDNA was transcribed from 2 μg of total RNA template in a 140-μl reaction mixture using a SYBR RT-PCR Kit (Takara Bio Co. Ltd., Otsu, Japan) with random hexamer. Real-time quantitative PCR was performed using Smart Cycler version II (Takara Bio Co. Ltd.) with the SYBR RT-PCR Kit (Takara Bio Co. Ltd.) according to the manufacturer's instructions, and intercalating SYBR Green I (Molecular Probes Inc., Eugene, Oregon) was detected. Assays were performed in duplicate, and the expression levels of target genes were normalized to expression of the glyceraldehyde-3-phosphate dehydrogenase (G3PDH) gene and hydroxymethylbilane synthase (HMBS), which is stable in the liver, as quantified using real-time quantitative PCR as internal controls. For accurate normalization, a set of two housekeeping genes was used in the present study. Sequences of primer sets were as follows:

RIG-I: 5'-AAAGCATGCATGGTGTTCCAGA-3',

5'-TCATTCGTGCATGCTCACTGATAA-3';

MDA5: 5'-ACATAACAGCAACATGGGCAGTG-3',

5'-TTTGGTAAGGCCTGAGCTGGAG-3';

LGP2: 5'-ACAGCCTTGCAAACAGTACAACCTC-3',

5'-GTCCCAAATTTCCGGCTCAAC-3';

Cardif: 5'-GGTGCCATCCAAAGTGCCTACTA-3',

5'-CAGCACGCCAGGCTTACTCA-3';

RNF125: 5'-AGGGCACATATTCGGACTTGTCA-3',

5'-CGGGTATTAAACGGCAAAGTGG-3';

ISG15: 5'-AGCGAACTCATCTTTGCCAGTACA-3',

5'-CAGCTCTGACACCGACATGGA-3';

USP18: 5'-TGGTTCTGCTTCAATGACTCCAATA-3',

5'-TTTGGGCATTTCCATTAGCACTC-3';

GAPDH: 5'-GCACCGTCAAGGCTGAGAAC-3',

5'-ATGGTGGTGAAGACGCCAGT-3'.

HMBS: 5'-AAGCGGAGCCATGTCTGGTAAC-3',

5'-GTACCCACGCGAATCACTCTCA-3'.

Sequential measurement of gene expression in PBMC before and during therapy

To understand transcriptional response of the genes to PEG-IFN alpha-2b and ribavirin therapy, serial expression of RIG-I, RNF125, Cardif, ISG15, and USP18 were determined before and during treatment in peripheral blood mononuclear cell (PBMC) in 14 patients (7 were SVR and 7 were NVR). PBMC was obtained from whole blood

samples collected before and at 4, 8, 24, 48, and 168 hours after the initiation of PEG-IFN alpha-2b and ribavirin combination therapy. After extraction of total RNA from the PBMC, the expression of mRNA was quantified at each specified time point using real-time quantitative PCR as described above. Gene expression levels at each time point during treatment were calculated relative to baseline expression levels measured prior to IFN treatment.

Western blotting

Western blotting was carried out in nine patients (five were SVR and four were NVR) and three non-HCV control subjects as described previously (22). Liver biopsy specimen of ~10 mg was homogenized in 100 μL of Complete Lysis-M™ (Roche Applied Science, Penzberg, Germany). Twenty micrograms of the homogenates were separated by SDS-PAGE and blotted onto a PVDF Western Blotting membrane. The membrane was incubated with the primary antibodies followed by a peroxidase-labeled anti IgG antibody, and visualized by chemiluminescence using the ECL Western blotting Analysis System (Amersham Biosciences, Buckinghamshire, UK). The anti-VISA mouse monoclonal antibody (BioDesign, Saco, ME) and anti-beta-actin antibody (Sigma, St. Louis, MO) were used.

HCV dynamics in serum

To analyze the viral dynamics, HCV-RNA was quantified just before and at 4, 8, and 24 hours, and 2, 7, 14, 28, 56, and 84 days after the initiation of PEG-IFN alpha-2b and ribavirin combination therapy, using real-time detection PCR, as reported previously (23). For each patient, the viral decline curve was plotted on a semilogarithmic scale,

and the slopes of the exponential viral declines were calculated for each viral decline phase with a straight-line fit of the data.

Definitions of response to therapy

A patient negative for serum HCV-RNA during the first six months after the completion of PEG-IFN alpha-2b and ribavirin combination therapy was defined as a sustained viral responder (SVR), and a patient for whom HCV-RNA became negative at the end of therapy and reappeared after completion of therapy was defined as a transient responder (TR). A patient who was positive for HCV-RNA even during the course of therapy was defined as a non-virological responder (NVR). HCV-RNA was determined with the Amplicor qualitative assay (Roche Molecular Diagnostics. Co., Tokyo, Japan). The detection sensitivity of this assay is approximately 50 IU/mL.

Statistical analysis

Categorical data were compared by the chi-square test and Fisher's exact test. Distributions of continuous variables were analyzed by Mann–Whitney U-test for two groups. Kruskal–Wallis test was used for multiple group comparisons. All tests of significance were two-tailed, and p values < 0.05 were considered statistically significant.

RESULTS

Patient characteristics

According to the final virological response, patients were classified into three groups: 30

were SVR, 24 were TR, and the remaining 20 were NVR, as shown in Table 1. Viral decline rates in NVR were significantly lower in both the first and second phases of HCV dynamics. It should be noted that most NVR patients exhibited no second-phase viral decline.

Data on factors that were available before starting the treatment were compared according to virological response by univariate analysis. As shown in Table 1, only age and platelet count were associated with viral response, and no other clinical factors were predictive of NVR before initiation of the therapy.

Gene expression involving innate immunity in the liver

First, we compared basal hepatic gene expression between the chronic hepatitis C patients (n = 74) and the non-viral liver disease patients (n = 5). As shown in Figure 1, levels of RIG-I, MDA5, LGP2, ISG15, and USP18 expression were significantly higher in the chronic hepatitis C patients than in the non-viral liver disease patients. However, there was no significant difference in levels of Cardif expression between the chronic hepatitis C and non-viral related liver disease patients.

Next, to assess the relationship between baseline hepatic gene expression and treatment efficacy, levels of gene expression were compared based on the final virological response. As shown in Figure 2, the hepatic expression level of RIG-I, MDA5, and LGP2 were significantly higher in NVR than in SVR and TR. In marked contrast, hepatic Cardif expression was significantly lower in the NVR group. The hepatic expression of RNF125, which is specific E3-ubiquitin ligase for RIG-I, MDA5, and

Cardif, was also significantly lower in the NVR group. Because negative correlation was found between RIG-I and Cardif or RNF125 expression, we calculated the ratio of RIG-I to Cardif or RNF125 expression levels. As shown in Figure 2, the difference among the groups was conspicuous when comparison was made with the RIG-I/Cardif ratio or RIG-I/RNF125 ratio. Moreover, the RIG-I/Cardif expression ratio before treatment was negatively and significantly correlated with the exponential viral decline rate in both the first and second phases of HCV dynamics (first phase, $r = -0.4$, $p < 0.0005$; second phase, $r = -0.5$, $p < 0.0001$). Similar correlation was found between RIG-I/RNF125 ratio and viral decline rate (first phase, $r = -0.4$, $p = 0.004$; second phase, $r = -0.2$, $p = 0.09$, data were not shown).

Like RIG-I and MDA5, intrahepatic expression levels of ISG15 and USP18 were significantly higher in NVR than in SVR and TR (Figure 2). When we assessed the correlation of these two genes in individual patients, we found a strong and significant correlation between ISG15 and USP18 ($r^2 = 0.88$, $p < 0.0001$). Levels of ISG15 and USP18 expression before treatment were negatively correlated with the exponential viral decline rates calculated from the first and second phases of HCV dynamics (ISG15, first phase, $r = -0.5$, $p < 0.0001$; ISG15, second phase, $r = -0.3$, $p = 0.02$; USP18, first phase, $r = -0.5$, $p < 0.0001$; USP18, second phase, $r = -0.3$, $p = 0.01$).

Receiver operator characteristic (ROC) analysis

To determine the usefulness of these gene quantifications as predictors, receiver operator characteristic (ROC) analysis was conducted (Figure 3). The area under the ROC curve (Az) for the RIG-I/Cardif ratio, ISG15, and USP18 was 0.91, 0.90, and 0.91,

respectively, suggesting that quantification of these gene transcripts is of use for the prediction of NVR (Table 2). In addition, this analysis also suggested that RIG-I/Cardif ratio would be more specific for prediction of NVR, whereas ISG15 and USP18 would be more sensitive (Table 2).

Multivariate analysis

Multivariate analysis for factors that were available before initiating therapy indicated that a higher ratio of RIG-I/Cardif and higher expression of ISG15 were independent factors that were associated with NVR (Table 3). In this analysis, USP18 was excluded because of its strong correlation with ISG15.

Protein levels of Cardif in the liver

Because hepatic expression of Cardif mRNA was significantly lower in NVR patients than in SVR patients, we determined the basal protein expression levels of Cardif in the liver in NVR and SVR patients. Western blot analysis demonstrated a single Cardif product in all samples (Figure 4A). Similar to Cardif mRNA expression, mean Cardif expression in NVR patients was significantly lower than that in SVR (Figure 4B, $p = 0.01$). The cleavage product of Cardif, which has been reported by Loo et al. (24), was not detected in our analyses.

Transcriptional responses to PEG-IFN alpha-2b and ribavirin therapy in PBMC

Sequential analysis in response to PEG-IFN alpha-2b and ribavirin demonstrated a rapid and strong induction of RIG-I, ISG15, and USP18 mRNA expression, which peaked 8 hours after PEG-IFN-alpha-2b administration (Figure 5). A greater fold change of these

peak inductions was observed in SVR patients compared with NVR patients, although statistical significance was not achieved. In marked contrast, RNF125 expression profile in response to PEG-IFN-alpha-2b was triphasic, and consisted of rapid and strong suppression peaked at 8 hours after administration, and increasing 1.5- to 2-fold above baseline level during 24–48 hours after the administration and gradually decreasing to baseline level (Figure 5). The rapid suppression and subsequent increase following PEG-IFN alpha-2b administration tended to have a greater fold change in NVR patients compared with those in SVR patients. In contrast from RIG-I, ISG15, USP18, and RNF125, Cardif expression profile was relatively constitutive, and transcriptional response to PEG-IFN was weak (Figure 5).

DISCUSSION

In the present study, we found that baseline expression levels of intrahepatic viral sensors and related regulatory molecules were significantly associated with the final virological outcome in patients with chronic hepatitis C who were treated with PEG-IFN alpha-2b and ribavirin combination therapy: up-regulation of RIG-I, MDA5, LGP2, ISG15, and USP18, and lower expression of Cardif and RNF125 could predict non-response to subsequent treatment with PEG-IFN alpha-2b and ribavirin. The positive predictive value of a high ratio of expression of RIG-I to Cardif (>0.88) for NVR was the highest at a value of 0.75 and the negative predictive values of high expression of ISG15 (>0.36/internal control) and USP18 (>0.67/internal control) were the highest at values of both 0.96. These data may be of use in predicting clinical responses to the PEG-IFN alpha and ribavirin combination before initiating therapy.